

# Suitability of granular carbon as an anode material for sediment microbial fuel cells

Jan B. A. Arends · Evelyne Blondeel ·  
Steve R. Tennison · Nico Boon · Willy Verstraete

Received: 24 August 2011 / Accepted: 9 May 2012 / Published online: 1 June 2012  
© Springer-Verlag 2012

## Abstract

**Purpose** Sediment microbial fuel cells (S-MFCs) are bio-electrochemical devices that are able to oxidize organic matter directly into harvestable electrical power. The flux of organic matter into the sediment is rather low; therefore, other researchers have introduced plants for a continuous supply of organic matter to the anode electrode. Until now only interconnected materials have been considered as anode materials in S-MFCs. Here, granular carbon materials were investigated for their suitability as an anode material in S-MFCs.

**Materials and methods** Laboratory microcosms with eight different electrode materials (granules, felts and cloths) were examined with controlled organic matter addition under brackish conditions. Current density, organic matter removal and microbial community composition were monitored using 16S rRNA gene PCR followed by denaturing gradient gel electrophoresis (DGGE). The main parameters investigated were the influence of the amount of electrode material applied to the sediment, the size of the granular material and the electrode configuration.

**Results and discussion** Felt material had an overall superior performance in terms of current density per amount of applied electrode material; felt and granular anode obtained similar current densities (approx. 50–60 mA m<sup>-2</sup>), but felt

materials required 29 % less material to be applied. Yet, when growing plants, granular carbon is more suited because it is considered to restore, upon disturbance, the electrical connectivity within the anode compartment. Small granules (0.25–0.5 mm) gave the highest current density compared to larger granules (1–5 mm) of the same material. Granules with a rough surface had a better performance compared to smooth granules of the same size. The different granular materials lead to a selection of distinct microbial communities for each material, as shown by DGGE.

**Conclusions** Granular carbon is suitable as an anode material for S-MFCs. This opens the possibility for application of S-MFCs in cultivated areas. In a wider context, the application of granular carbon electrodes can also be an option for in situ bioremediation of contaminated soils.

**Keywords** 16S rRNA gene · Bio-energy · Electron transfer · In situ bioremediation · Wetlands

## 1 Introduction

Microorganisms are able to reduce solid materials (mostly metal-(hydr)oxides) while oxidizing organic carbon in the soil. This phenomenon of microbial respiration has successfully been applied to construct microbial fuel cells (MFC) (Logan et al. 2006). These devices consist of an anaerobic compartment where microbes are able to oxidize organic matter while delivering electrons to a solid electrode. These electrons are passed through an external circuit and end up in the cathode compartment in a final reduction reaction. The compartments are physically separated by means of an ion exchange membrane to ensure electro-neutrality and prevent the crossover of reactants. These reactor configurations enable direct electrical power recovery from a wide

---

Responsible editor: Gijs Breedveld

---

J. B. A. Arends · E. Blondeel · N. Boon · W. Verstraete (✉)  
Faculty of Bioscience Engineering, Ghent University,  
Coupure Links 653,  
9000 Gent, Belgium  
e-mail: Willy.Verstraete@UGent.be

S. R. Tennison  
Mast Carbon International Ltd.,  
Basingstoke, Hampshire RG22 4BA, UK

range of liquid streams, e.g. wastewater (Aelterman et al. 2006). Power densities obtained in these types of reactor systems reach values of 10–100  $\text{W m}^{-3}$  (Aelterman et al. 2006). Current densities range from as low as 4  $\text{mA m}^{-2}$  to 2  $\text{A m}^{-2}$  (Pant et al. 2010). The MFC has been successfully applied to waterlogged sediment systems. Here, the anode is placed in the anaerobic sediment layer, and the (biological) oxygen reducing cathode is floating in the water above. The membrane is not installed, but its function is maintained by the sediment layer on top of the anode. This easy-to-maintain system has been developed in marine settings (e.g. Reimers et al. 2001), but later freshwater systems were also tested (e.g. Holmes et al. 2004; Mohan et al. 2009). The sediment MFC (S-MFC) is the first MFC design that has been reported with a useful application, mainly powering different types of remote sensors (meteorological buoy etc.; Tender et al. 2008). Typical peak power outputs obtained with unmodified anodes are 0.2–55  $\text{mW m}^{-2}$  (Scott et al. 2008) whereas current densities can amount to 100  $\text{mA m}^{-2}$  before mass transport becomes limiting (Scott et al. 2008). Note that waterlogged soils are also applicable for anode placement. Here, the word ‘sediment’ will be used to indicate both material types.

Applications were gradually expanded from marine environments into brackish and freshwater environments; however, the flux of organic matter towards the anode still remains rather low. A major portion (20–60 %) of the net fixed organic carbon during photosynthesis can be deposited in the soil as rhizodeposits (i.e. dead root biomass, active secretions or diffusive leakage) (Neumann and Römheld 2007). Therefore, a planted sediment microbial fuel cell (P-MFC) has the potential to provide long-term sustained power output due the continuous photosynthetic activity of the plant. Indeed, several research groups found that planting sediment fuel cells resulted in more power and current output. Rice plants (*Oryza sativa*) were used in sediment type fuel cells (De Schamphelaire et al. 2008; Kaku et al. 2008) while reed mannagrass (*Glyceria maxima*) and common cordgrass (*Spartina anglica*) were used in a reactor-type system containing a membrane and a separate cathode (Strik et al. 2008; Timmers et al. 2010). Comparing planted with non-planted S-MFC, De Schamphelaire et al. (2008) found a seven-to-ninefold increase in power density and a threefold increase in current density of the planted systems vs the non-planted systems amounting to 33  $\text{mW m}^{-2}$  sustained power production (De Schamphelaire et al. 2008).

Until now, the P-MFC has mostly been explored in reactor type settings with the anode compartment completely filled with electrode material, either cloth or granular carbon (e.g. De Schamphelaire et al. 2008; Strik et al. 2008; Helder et al. 2010). S-MFCs have only been researched with solid connected materials such as carbon or stainless steel felts, cloths, rods etc. (e.g. Reimers et al.

2001; Dumas et al. 2008; Scott et al. 2008; Tender et al. 2008; Jian-hai et al. 2009). In order to make a P-MFC widely available, for instance in greenhouses or (cultivated) wetlands, there is a need for granular material that can readily interact with the roots but is not irreversibly damaged when agricultural practices are applied. One should be able to plant or harvest in such matrices. Granular materials are easily mixed with sediments and are able to create new connections after disturbance of the packed bed. Felt or cloth materials can be easily damaged but are not readily reconnected. Solid materials are not easily damaged but do not provide a large surface area for interaction with the plant and the electro-active microorganisms and may also hamper agricultural practices. In this study, a range of carbon materials were tested in microcosms to investigate the suitability of the use of granular materials as an anode material for P- and S-MFC. Parameters such as the amount of electrode material, the electrode configuration (loose or interconnected) and the granule size have been taken into account.

## 2 Materials and methods

### 2.1 Experimental setup

Glass jars with a volume of 350 ml were used for these studies (Fig. 1). Various anode materials were mixed with a layer of sand (Table 1). Materials were used as supplied, except for M1a which was washed with tap water to remove the dust. Cloth and felt materials had a projected area of  $4 \times$

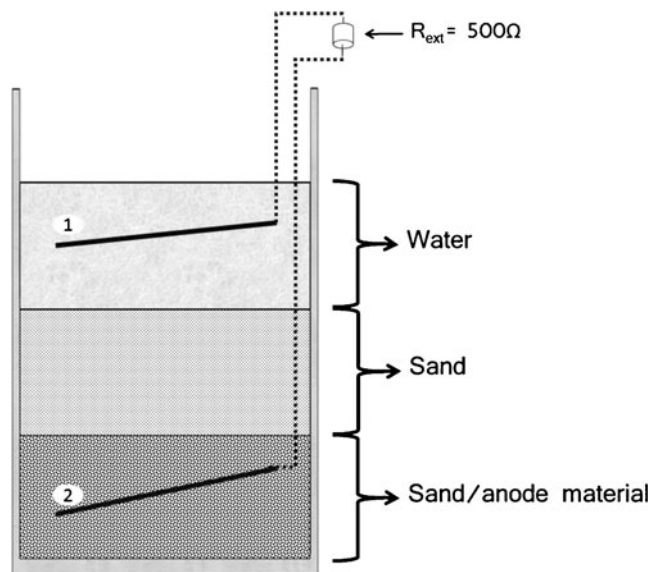


**Fig. 1** Schematic of the sediment microcosms used for the testing of various anode materials. 1 Graphite rod connected to graphite felt acting as cathode. 2 Graphite rod current collector connecting the anode materials under study to the 500- $\Omega$  resistor. Electrical connection: .....

4 cm<sup>2</sup>, and one layer, interwoven with a graphite rod (5-mm diameter; Morgan, Belgium) as a current collector, was placed in the anode compartment. Granular material was mixed in a 1:1 volume ratio with sand (70.5 wt%=0.25–0.5-mm diameter, pH=9.9 in 1:10 dilution). A graphite rod was introduced in the middle of the sand/granule layer, at the same position as the cloth materials. In this paper, the AR-value refers to the percentage of volume of the anode compartment which is occupied by the electrode material, e.g. a ratio of 1:1 corresponds to AR-50. To accommodate different percentages of felt material, more layers were added to the current collector. The same volume of sand was placed on top of the anode, which can be considered a membrane, followed by an equivalent volume of liquid. M9 medium modified with 13 g l<sup>-1</sup> NaCl and 14.7 mg l<sup>-1</sup> CaCl<sub>2</sub> was used in all tests (Rabaey et al. 2005); therefore, the microcosms can be considered brackish at pH 8, ensuring a good conductivity and no pH inhibition of the anode (Logan et al. 2006). In this work, no plants were used, because varying rhizodeposition patterns and plant/microbe interactions might obscure outcomes directly related to the materials under study. Instead, organic carbon was provided as 20 mM of COD (chemical oxygen demand), in the form of sodium acetate, in the liquid of the anode compartment at the start of the experiment. This corresponds to about 2.5 ton dry matter ha<sup>-1</sup> on the assumption that 70 % of organic dry matter is COD. For the long-term test, 100 mM COD (12.5 ton dry matter ha<sup>-1</sup>) was added (1:1 mix of sodium acetate and starch). To maintain current productivity, COD additions in the form of a concentrated stock solution of COD in M9 were injected at random places with a syringe when the current dropped. To provide electroactive microorganisms, and thus ensure a fast start-up of the S-MFC, 5 vol% effluent of an acetate oxidizing anode (operated in the laboratory for over a year) was added to the anode compartment at the start of the incubation (Clauwaert et al. 2007b). Cathodes were 3×4 cm<sup>2</sup> carbon felts (see Table 1) incubated in the recirculation liquid of an oxygen-reducing biocathode operated in the laboratory for over a year (Clauwaert et al. 2007b). To counteract evaporation, cathodes were replenished with distilled water when needed. All incubations were conducted in duplicate at room temperature (22±2 °C).

## 2.2 Electrochemical monitoring and chemical analysis

Cell potential over a 500-Ω resistor and anode or cathode potential vs an Ag/AgCl reference electrode (BASi Inc., UK) were measured continuously (Agilent benchlink datalogger). The reference electrodes were regularly monitored versus a calomel electrode (+244 mV vs Normal Hydrogen Electrode (NHE); QIS, the Netherlands). Polarization curves were recorded with a Bistat potentiostat (Biologic, France) at a scan rate of 1 mV s<sup>-1</sup> following a 20-min stabilization

period in open circuit. Electrochemical calculations were performed according to Logan et al. (2006). Current and power densities are reported normalized to the total surface area of the microcosm (0.0034 m<sup>2</sup>).

Alternative electron acceptors (NO<sub>2</sub><sup>-</sup>, NO<sub>3</sub><sup>-</sup> and SO<sub>4</sub><sup>2-</sup>) were determined by ion chromatography as described previously (Clauwaert et al. 2007a). Chemical oxygen demand was determined by means of a standard kit according to the manufacturer's procedures (Macherey-Nagel, Germany). Samples from the anode compartment were taken at random places.

## 2.3 Microbial community and material structure analysis

Samples from the sand, and sand mixed with M1a, M1b and M2, were taken at the end of the long-term incubation (55 days) for analysis of the bacterial community structure (1 ml sediment and 1 ml pore liquid) and for scanning electron microscopy (SEM) (1 ml sediment). Samples were taken from at least five random positions per microcosm in order to obtain a homogenous, representative sample. Total DNA was extracted (Boon et al. 2000) followed by amplifying the bacterial 16S rRNA gene with primers 338F-GC and 518R. The different amplicons were separated using denaturing gradient gel electrophoresis (Carballa et al. 2011). The obtained profiles were clustered using BioNumerics software v5.1 (Applied Maths, Belgium). Theoretical ecological parameters—range weighted richness (Rr; a measure of habitability of an environment) and community organization (Co; an approximate of functional diversity)—were attributed according to the microbial resource management (MRM) toolbox (Read et al. 2011). Samples for SEM were immediately fixed by subsequent incubation in 2.5 % glutaraldehyde (2 h) and 1 % osmium tetroxide (1 h) with three times washing with 0.1 M phosphate buffer (pH 7.5) in between. Subsequent dehydration was done with 30, 50, 70, 90 and 3×100 % ethanol (20 min per step) followed by overnight drying in a desiccator.

## 3 Results

### 3.1 Initial material screening

Eight different materials (see Table 1) were screened for their ability to receive electrons from an electro-active microbial community in a sediment setting for about 10 days. From this initial screening, the big granules with a diameter of 1–5 mm (M1a) gave the best performance (90 C transferred), followed by all the felt/cloth materials (M4–M8) which gave about the same number of total coulombs transferred for all different materials (20–40 C). The least

**Table 1** Materials used in this study

Material code	M1a	M1b	M2	M3	M4	M5	M6	M7	M8
Supplier	Mersen	Mersen	MAST	MAST	Alfa Aesar	MAST	MAST	MAST	MAST
Properties									
Form	Granules	Granules	Beads <sup>a</sup>	Beads <sup>a</sup>	Felt	Felt	Felt	Cloth	Cloth
Precursor	Phenolic resin and polymers	M1a	Phenolic resin	Phenolic resin	Resin	Viscose fiber	Viscose fiber	Viscose fiber	Viscose fiber
Size (mm)	Diameter				Thickness			Fiber diameter	
	1–5	0.25–0.5	0.25–0.5	0.25–0.355	3.18	1.5	2.5	0.01–0.005	0.01–0.005
Density	kg l <sup>-1</sup>				g m <sup>-2</sup>				
	1.8 <sup>b</sup>	0.8	2.6	0.5	240	118	–	180	100
BET surface area (m <sup>2</sup> g <sup>-1</sup> )	0.5–1.3	–	1374	553	2	1231	365	900–1100	900–1100
Elemental composition									
C atom (%)	96.97	–	97.2	97.5	> 99	–	–	–	–
O atom (%)	3.03	–	1.8	1.7	–	–	–	–	–
N atom (%)	/	–	1	0.8	–	–	–	–	–
Potential of zero charge (pH)	–	–	> 10	> 10	–	> 10	> 10	> 10	> 10
Remark	Amorphous remainder of electrographite production	Ground M1a granules	Smooth porous bead, highly mesoporous core, 38–40 % activated to create a high microporosity	Smooth porous bead, highly mesoporous core, not activated, therefore has limited microporosity	–	~ 30 % activated	Carbonized	Knitted, ~ 30 % activated	Knitted, ~ 30 % activated

Data as supplied by the different companies in personal communication or in publically available product data sheets. Mersen; Wommel, Belgium. Alfa Aesar; Karlsruhe, Germany

Solidus (/) indicates not detected; en dash (–) indicates not available

BET Brunauer–Emmet–Teller

<sup>a</sup>Beads possess identical chemistry but a lower porosity as described in Tripisciano et al. (2011)

<sup>b</sup>Determined by Clauwaert et al. (2007a)

performing materials were the small granular carbon materials with a diameter <0.5 mm (M2 and M3; 7–11 C) (Fig. 2).

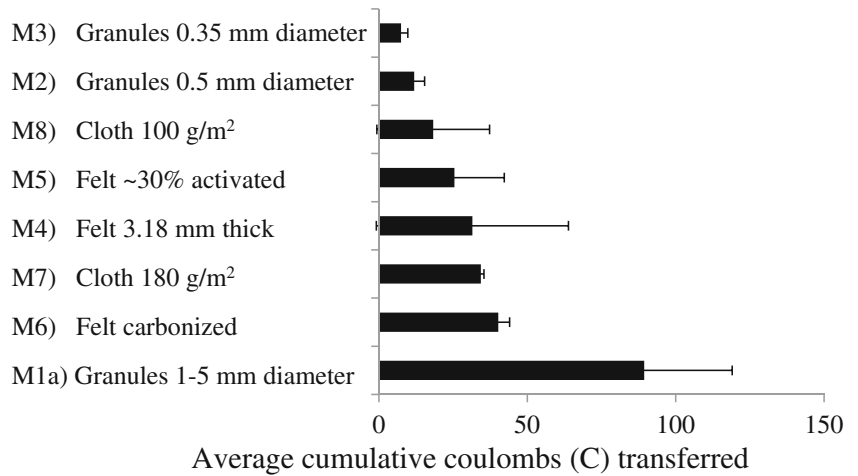
### 3.2 Influence of particle size

The initial experiment indicated that particle size had a large influence on electron transfer capabilities within the anode. It was hypothesized that a certain size distribution in relation to the sand is optimal for electrical connectivity in the soil or sediment. To investigate this further, the large granules (M1a) were ground to smaller particles. From this ground material, the particles in the range of 0.25–0.50 mm were selected (M1b). Both materials (M1b and M2) had the same size as the major fraction of the sand. At an AR-50, the ground particles were compared to the original particles of 0.25–0.50 mm (M2), the large 1–5-mm particles (M1a) and a graphite rod only. After 3 weeks of incubation, electrical current densities averaged  $55.2 \pm 11.7$  mA m<sup>-2</sup> with a maximum of  $77.7$  mA m<sup>-2</sup> for the ground granules (M1b). The 1–5-mm granules (M1a) reached an average current density of  $25.2 \pm 7.74$  mA m<sup>-2</sup> with a maximum of  $37.9$  mA m<sup>-2</sup>.

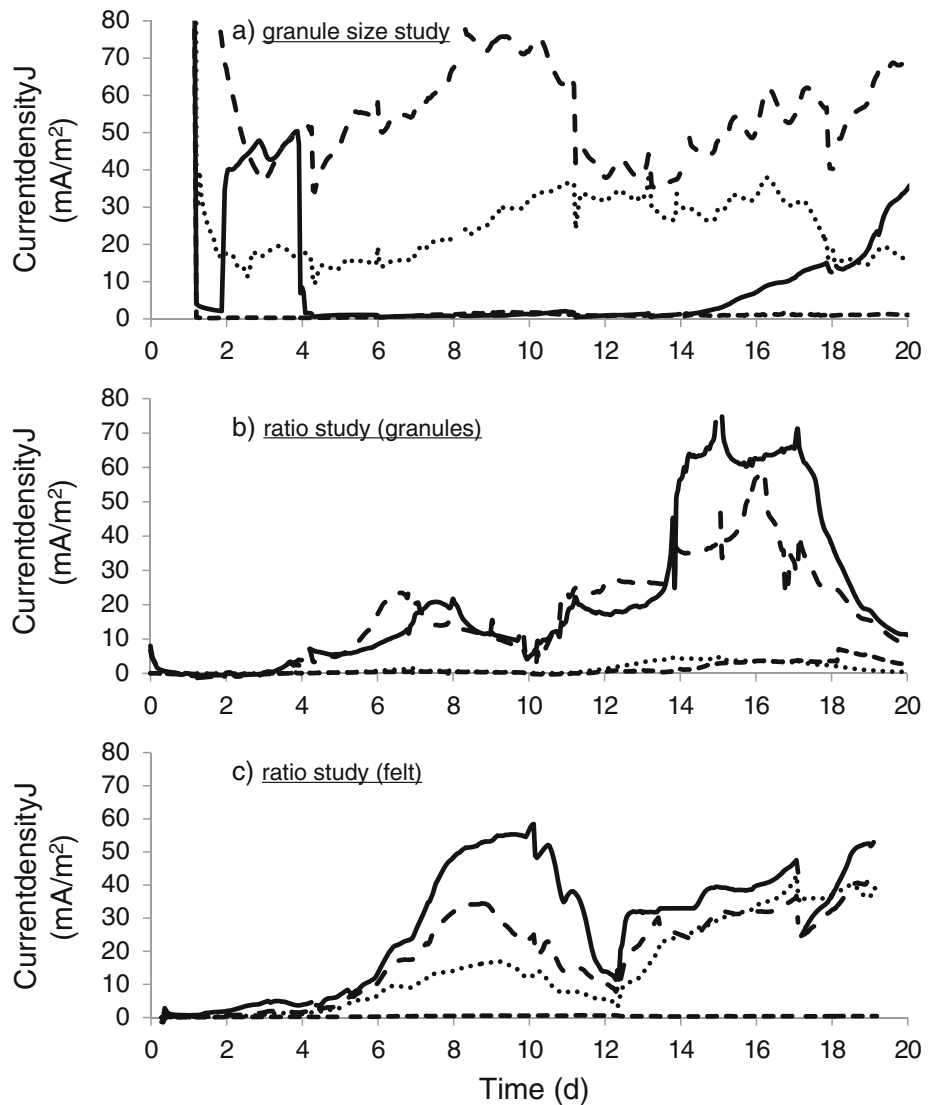
The original small granules (M2) averaged  $5.33 \pm 7.9$  mA m<sup>-2</sup> with a maximum of  $35.4$  mA m<sup>-2</sup> (Fig. 3a). The microcosm with only the rod as the current collector averaged  $1.01 \pm 0.37$  mA m<sup>-2</sup> with a maximum of  $1.87$  mA m<sup>-2</sup>. The results of the sustainable current production were corroborated by the maximum current densities obtained during the forward sweep of a polarization curve;  $140.1 \pm 42.4$  mA m<sup>-2</sup>,  $38.8 \pm 10.4$  mA m<sup>-2</sup> and  $8.0 \pm 6.4$  mA m<sup>-2</sup> were the average maximum current densities obtained during this time period for M1b, M1a and M2, respectively. As current densities are the result of both anodic and cathodic processes, an examination of the anode potential is needed.

The minimum anode potentials, as determined from the open circuit potential from the polarization curves, indicated that all materials (rod, M1a and M1b) except for M2 were able to reach a low anode potential, i.e.  $-0.067$  till  $-0.185$  V vs NHE at day 18. The anode potential of M2 varied around  $+0.2$  V vs NHE (Fig. 4b). The low anode potentials found here correspond to an anoxic environment with COD oxidation as normally found in anodes of MFC (Logan et al.

**Fig. 2** Initial screening of various materials shows that bigger granules (1–5 mm) transferred more coulombs, followed by felt/cloth materials and smaller granules (0.25–0.50 mm). The error bars indicate standard deviation ( $n=2$ )



**Fig. 3** Current density profiles over time. **a** Granule size study: 1–5 mm (M1a) (·····), 0.25–0.50 mm (M1b) (---), 0.25–0.50 mm (M2) (—), rod only (---). **b** Application ratio study 1–5-mm granules (M1a): AR-0 (---), AR-33 (·····), AR-67 (---), AR-100 (—). **c** Application ratio study 3.18-mm felt (M4): AR-0 (---), AR-14 (·····), AR-28 (---), AR-42 (—). Data for all tests are averaged for duplicate experiments performed at the same time except for AR-42 felt M4 (3C) which is data from a single experiment. Sudden changes in the graphs are due to manipulations such as polarization curves, sampling or addition of distilled water to the cathode





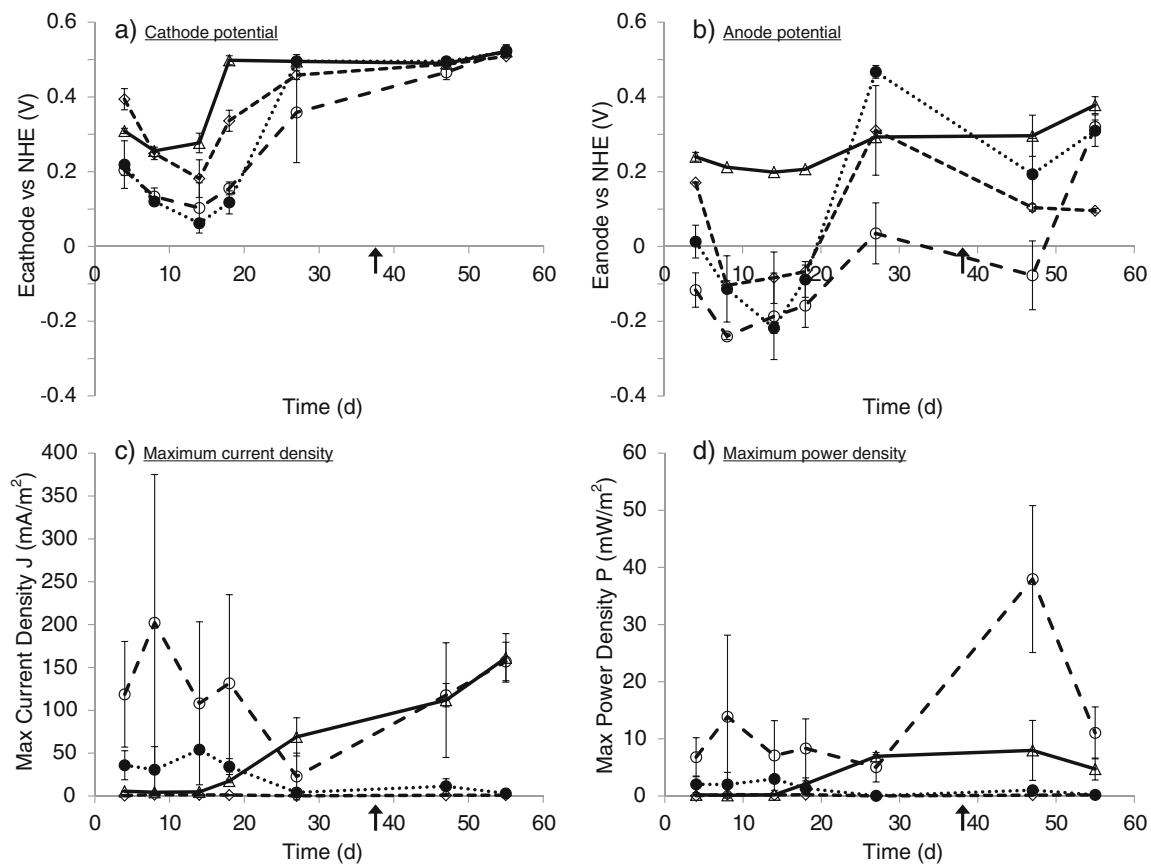


**Fig. 4** Open circuit cathode (a) and anode (b) potential over time during granule size study as measured before a polarization curve. Maximum current density, i.e. current at short circuit (c) and maximum power as measured during the forward sweep of the polarization curve

(d): 1–5 mm (M1a) (●—), 0.25–0.50 mm (M1b) (○—), 0.25–0.50 mm (M2) (△—), no material, only the current collector (◇—). Error bars indicate standard deviation, sometimes smaller than the symbol ( $n=2$ ). Arrow indicates addition of COD

2006). The higher anode potential corresponds with the low current density as indicated earlier (see Fig. 3a).

### 3.3 Influence of application ratio

As the above described tests were conducted at AR-50, a follow-up experiment was performed to understand the influence of various application ratios on the current density. These tests were conducted for the large granules 1–5 mm (M1a; i.e. the best performing granular material) and for the 3.18-mm felt (M4; a randomly selected felt/cloth material). For the large granules (M1a), the same current density profile over time could be distinguished for AR-67 and AR-100. The maximum current density obtained was, however, 59.3 mA m<sup>-2</sup> for AR-67, while AR-100 obtained a value of 74.8 mA m<sup>-2</sup> (see Fig. 3b). This coincides with the previous test where AR-50 only reached a maximum current density of 37.9 mA m<sup>-2</sup> (see Fig. 3a). The felt material test showed an initial clear difference between the different sand/felt application ratios; the higher the amount of felt, the higher the resulting current density. However, addition

of COD (day 12.5; Fig. 3c) resulted in a similar current density profile (39.6–52.9 mA m<sup>-2</sup>, see Fig. 3c) for ratios AR-14, AR-28 and AR-42. The highest application ratio still had the highest current density, but the other ratios increased considerably in current density after addition of COD. As COD was randomly applied by means of a concentrated solution distributed with a syringe, the effect of supplying COD locally can be clearly seen. This indicates that the system was rather substrate-limited starting from day 10. This coincides with the practical implication that the electrode needs to be near the source of COD for a sustained current generation in sediment systems (Scott et al. 2008).

### 3.4 Long-term incubation

The short-term experiment as described in “Section 3.2” was extended over a longer time period. The microcosms with the small granules (M2) were able to produce a sustainable current, comparable to the ground granules (M1b). This was, however, mostly due to an increase in cathode potential for M2 (see Fig. 4a). The anode potential remained

positive as seen during the short-term incubation (see Fig. 4b). It even rose by 0.164 V to +0.378 V vs NHE at day 55. The cathode potential increased over the same time period by 0.187 V to 0.521 V vs NHE. The most striking observation that could be made from the long-term data is that the small granules (M2) were not able to obtain a low anode potential, which is necessary for long-term sustainable current production, whereas the other materials were able to maintain anode potentials of about  $-0.2$  V vs NHE when COD was present. The correlation of a low anode potential with COD was observed during the long-term incubation where addition of COD resulted in a lowering of the anode potential in open circuit (see Fig. 4b). Adding extra COD did not result in a lower anode potential for material M2. Interestingly, the maximum current that was measured at the end of the forward sweep of the polarization curves of M1b and M2 showed similar patterns over time (see Fig. 4c). Although the maximum current densities were similar between M1b and M2 after 20 days of incubation, the maximum power output was considerably different (see Fig. 4d). M1b had a maximum power output of  $37.9 \pm 12.9$  mW m<sup>-2</sup>, whereas M2 had a maximum power output of  $8.0 \pm 5.2$  mW m<sup>-2</sup>. From these numbers the influence of the higher anode potential can be distinguished as this leads to a lower cell potential and thus a lower power density, although similar maximum current densities were achieved.

### 3.5 Organic carbon removal

Chemical oxygen demand (COD) removal efficiencies were determined based on total added COD and produced current. At the end of the short-term experiment that investigated the effect of granule size, the highest removal efficiency, 46.5 %, was found for the ground granules (M1b), followed by the big granules (M1a; 27.1 %) and the small granules (M2; 9.6 %). The microcosm with only a rod as a current collector obtained a COD removal efficiency of 5.2 %. At the end of the application ratio test for the large granules (M1a), COD removal efficiencies were about equal for AR-67 and AR-100, i.e. 9.8 % and 12.1 %, respectively. AR-0 and AR-33 obtained COD removal efficiencies of 0.71 % and 0.77 %, respectively. For the felt material (M4), COD removed as current was 14.9 %, 10.0 % and 8.1 % of the total added COD for AR-42, AR-28 and AR-14, respectively. These overall low removal efficiencies indicate that most organic carbon was removed through an alternative pathway, other than current production. This can be through methanogenesis or by oxidation using an alternative electron acceptor such as residual O<sub>2</sub>, NO<sub>3</sub><sup>-</sup> or SO<sub>4</sub><sup>2-</sup>. As the potential of the anodes indicated anaerobic conditions and there were no N-electron acceptors present (i.e. NO<sub>2</sub><sup>-</sup>, NO<sub>3</sub><sup>-</sup>), and because SO<sub>4</sub><sup>2-</sup> could have accounted maximally for 16 % of added COD (under the assumption

of complete reduction to H<sub>2</sub>S), it is hypothesized that methane production was the dominant competing mechanism. The latter gas could not, however, be monitored in this setup.

### 3.6 Microbial community and material structure

At the end of the long-term incubation, samples were analysed for their constituent microbial community based on 16S rRNA gene profiles using DGGE analysis. The results indicated that the type of material had a major influence on the type of microbial community that finally developed. All microbial communities were considerably different from the original electrogenic inoculum, due to the different circumstances experienced in the sediment as compared to the reactor type anode. The communities most similar to the original inoculum were the ones found in the incubations with M1b, with Pearson correlations of 36.2 and 52.5 %. The indigenous sand microbial community was not related to the electrogenic inoculum (0 % Pearson similarity). The small ground granules (M1b) had developed a distinct microbial community which could be readily differentiated from the communities on the precursor material (M1a) and on the small granules from another source (M2) (Fig. 5). Applying ecological parameters to these microbial community profiles shows that the range-weighted richness (Rr) is highest for M1b, followed by M1a, while M2 shows the lower Rr values.

The community organization (Co) of the microcosms indicated that M2 has the highest value indicating that these microcosms were dominated by a few species whereas the other microcosms were able to sustain a more evenly distributed microbial community. The dominant organism present in the electrogenic inoculum was also found in the best performing microcosms, i.e. containing M1b (identified by the arrow in Fig. 5). An organism that was present in the sand was able to colonize the carbon materials abundantly (identified by the arrowhead in Fig. 5). Interestingly, a dense biofilm was not present on any of the granular materials (Fig. 6). A striking difference could be observed in microbial localization on the electrode material. The microorganisms seemed to prefer to attach to surface imperfections. As the porous bead material M2 had only few of these surface imperfections compared to M1a and M1b, less interaction between the COD (electron donor), microorganisms and the electrode material (electron acceptor) was possible.

## 4 Discussion

Two parameters influenced the performance of granular carbon materials as anodic electrodes in S-MFC. The first important property was the granule size; smaller granules of

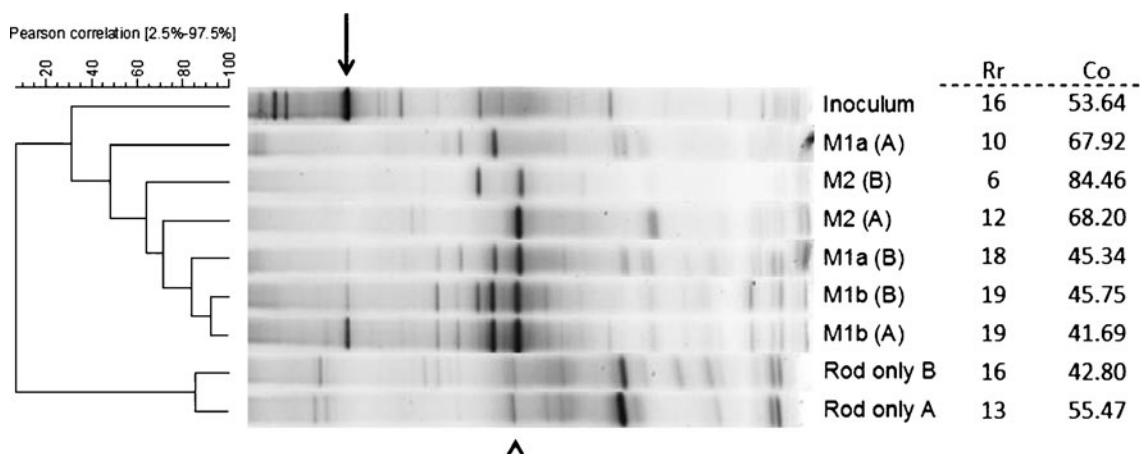


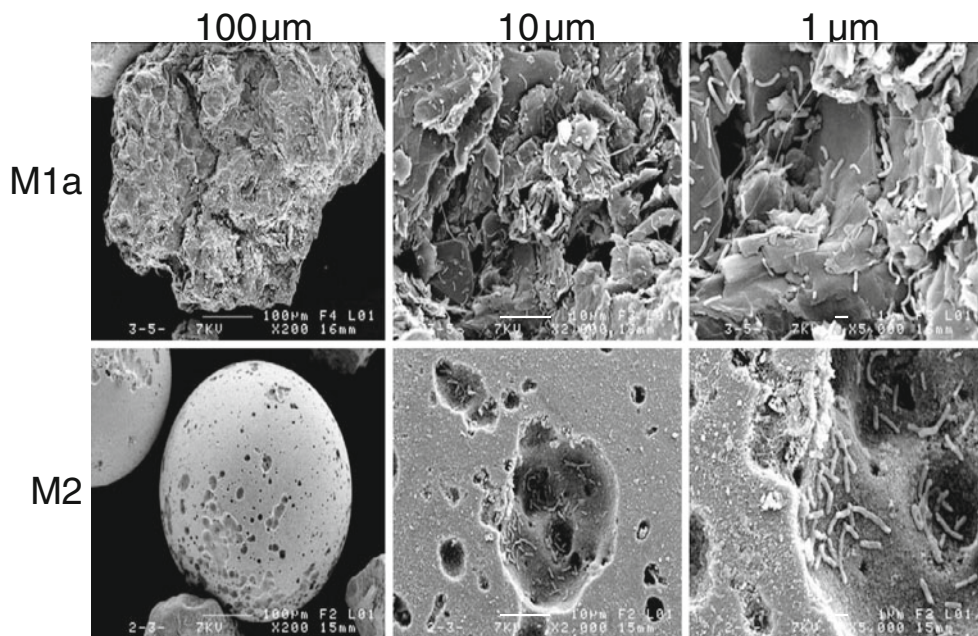
**Fig. 5** Pearson correlation clustering of 16S rRNA gene bacterial PCR products separated on DGGE. Capital *A* or *B* indicates duplicate microcosms. Rod only: no electrode material, only a current collector was present (i.e. community profile is representative for the sand used). *Rr* bacterial

richness, *Co* community organization. *Arrow*: dominant microorganism in the inoculum. *Arrowhead*: non-dominant microorganism in the sand capable of colonizing anode electrodes

the same material resulted in a higher performance, i.e. max 77.7 mA m<sup>-2</sup> for M1b vs 37.9 mA m<sup>-2</sup> for M1a under sustainable current operation. Aelterman et al. (2008) examined different sized granular material as an anode electrode in a packed bed configuration in a reactor type MFC. They did not find any difference in current producing performance between the different granule sizes. They worked with a completely packed bed, while in this study the sand particles were able to interfere with the electrical connectivity between the individual granules. Aspects of specific surface, electrical connectivity and tortuosity (i.e. path length of electron movement) and internal resistance need to be explored further with respect to the overall electrical conductivity in the soil.

The second important property is the intrinsic characteristics of the material itself, since the same sized materials, but from different precursors, resulted in differing current densities. More markedly, the difference could be seen in the overall anodic potential that was maintained during the incubation. As M2 was made from scratch by carbonizing precursor beads, this material has a highly defined surface structure and internal porosity (see Table 1). Materials M1a and M1b were made of scrap carbon with less defined structural properties, and M1b had, due to additional grinding, a more amorphous nature to the outer surface. The surface structure as examined by SEM had a major influence on where the microorganisms were able to respire with this solid electron acceptor (see Fig. 6). The microbial community present on the

**Fig. 6** Scanning electron microscope (SEM) examination of material structure and interaction with microorganisms. For details on M1a and M2, see Table 1. Sizes refer to scale bars in the picture





electrode material also showed distinct differences in their respective community structures. This can be related to the different electrode materials and can thus explain why the rough material (M1a and M1b) had a better performance in terms of anode potential and thus overall power output. Various theoretical ecological parameters and also visual inspection of the DGGE profile show that M2 creates a more selective environment or a niche environment that excludes important members of the initial electrogenic microbial community. The high anode potential of M2 can possibly be related to trapped oxygen within the highly microporous beads. This means that the microorganisms were able to respire with oxygen, not at the cathode but inside the anode. This idea leads to the new hypothesis that oxygen-containing beads might enhance in situ bioremediation (see below) through bio-electrochemical removal of pollutants on the outside of the beads. This hypothesis of oxygen trapped inside the beads being the cause for the high anode potential could, however, not be unequivocally elucidated during this study and thus warrants further in-depth analysis.

The use of granular electrode materials for P-MFC has been described previously only in packed bed configurations. De Schamphelaire et al. (2008) noted that the performance of this configuration was inferior as compared to felt mixed with soil. On the other hand, Timmers et al. (2010) have noted a good performance with materials from the same supplier as used in this work (M1). Both authors have used different types of plants in their research which might be the cause for the differing performances. The presence of soil can thus enhance current output in a P-MFC, which justifies mixing the granular electrode with the soil while at the same time creating a high surface area for interaction with plant roots and electroactive microorganisms. Current densities obtained during previous research fit with the current densities as seen during this study. Timmers et al. (2010) obtained  $84 \pm 70$  and  $141 \pm 52$  mA m<sup>-2</sup> with their *S. anglica* MFCs with a packed bed of granules in the anode. De Schamphelaire et al. (2008) were able to obtain a sustainable current density of 120 mA m<sup>-2</sup> with *O. sativa*. For non-planted S-MFC, current densities are usually smaller than for P-MFC (Scott et al. 2008; Zhang et al. 2010). This leads to the observation that current densities obtained in this study with granular carbon anodes are comparable to those in previous work and are possibly limited by the supply of reactants to and from the anode instead of the anode configuration (Scott et al. 2008).

From a current density perspective, the felt materials seem to be the better choice because with smaller amounts (lower AR value) higher current densities can be obtained compared to granular materials. However, taking also the use of plants and possible agricultural practices into account, this study has shown that granular materials can provide a good alternative. MFC technology has been

proposed as a means of alternative or enhanced soil or sediment remediation (Williams et al. 2010; Yuan et al. 2010; Zhang et al. 2010). The idea behind this concept is to provide an extra electron donor or acceptor in the form of an electrode. This electrode can also be inoculated with useful microorganisms. Until now MFC technology was only able to work locally in the soil/sediment; there was little convection, and mass transport was diffusion dominated (Scott et al. 2008). Using a loose, granular anode electrode as opposed to a solid rod or block can provide more degrees of freedom to manipulate the soil or sediment. The anode will not be damaged, merely rearranged and thus increasing the effective working range for a bioremediation process.

## 5 Conclusions

In this work, it was shown that granular carbon is able to function as an anode electrode in a sediment microbial fuel cell (S-MFC). For the particular materials in this study, it was found that an application ratio of 67 % in the soil was most beneficial for the granular material in terms of current output. The application ratio and type of material have a major influence on the resulting current density that can be obtained from the particular S-MFC under investigation. Further work is warranted to better optimise and understand the influence of different materials in combination with different soils on the resulting current density. The effect of the electrode material on the biology present (e.g. microorganisms) needs to be taken into account before this concept can be taken into the field and be applied as a power generation system, or for enhancing in situ bioremediation.

**Acknowledgments** This research received funding from the European Community Seventh Framework Programme FP7/2007-2013 under grant agreement no. 226532. The authors gratefully acknowledge Matthieu Picot, University de Rennes 1, for help with SEM analysis. Tim Lacoere is thanked for help with the molecular biological analysis. The authors thank Jo de Vrieze and Carlos Zamalloa for helpful suggestions and fruitful discussions.

## References

- Aelterman P, Rabaey K, Clauwaert P, Verstraete W (2006) Microbial fuel cells for wastewater treatment. *Water Sci Technol* 54:9–15
- Aelterman P, Versichele M, Marzorati M, Boon N, Verstraete W (2008) Loading rate and external resistance control the electricity generation of microbial fuel cells with different three-dimensional anodes. *Bioresour Technol* 99:8895–8902
- Boon N, Goris J, De Vos P, Verstraete W, Top EM (2000) Bioaugmentation of activated sludge by an indigenous 3-chloroaniline-degrading *Comamonas testosteroni* strain, I2gfp. *Appl Environ Microbiol* 66:2906–2913

- Carballa M, Smits M, Etchebehere C, Boon N, Verstraete W (2011) Correlations between molecular and operational parameters in continuous lab-scale anaerobic reactors. *Appl Microbiol Biotechnol* 89:303–314
- Clauwaert P, Rabaey K, Aelterman P, De Schampheleire L, Ham TH, Boeckx P, Boon N, Verstraete W (2007a) Biological denitrification in microbial fuel cells. *Environ Sci Technol* 41:3354–3360
- Clauwaert P, Van der Ha D, Boon N, Verbeken K, Verhaege M, Rabaey K, Verstraete W (2007b) Open air biocathode enables effective electricity generation with microbial fuel cells. *Environ Sci Technol* 41:7564–7569
- De Schampheleire L, van den Bossche L, Dang HS, Hofte M, Boon N, Rabaey K, Verstraete W (2008) Microbial fuel cells generating electricity from rhizodeposits of rice plants. *Environ Sci Technol* 42:3053–3058
- Dumas C, Mollica A, Feron D, Basseguy R, Etcheverry L, Bergel A (2008) Checking graphite and stainless anodes with an experimental model of marine microbial fuel cell. *Bioresour Technol* 99:8887–8894
- Helder M, Strik DPBTB, Hamelers HVM, Kuhn AJ, Blok C, Buisman CJN (2010) Concurrent bio-electricity and biomass production in three plant-microbial fuel cells using *Spartina anglica*, *Arundinella anomala* and *Arundo donax*. *Bioresour Technol* 101:3541–3547
- Holmes DE, Bond DR, O'Neil RA, Reimers CE, Tender LR, Lovley DR (2004) Microbial communities associated with electrodes harvesting electricity from a variety of aquatic sediments. *Microb Ecol* 48:178–190
- Jian-hai L, Yu-bin F, Jia L, An-long L, Dong-dong M (2009) Effect of electrode shape on power and internal resistance in benthic microbial fuel cell material on marine sediment. *Adv Mat Res* 79–82:2195–2198
- Kaku N, Yonezawa N, Kodama Y, Watanabe K (2008) Plant/microbe cooperation for electricity generation in a rice paddy field. *Appl Microbiol Biotechnol* 79:43–49
- Logan BE, Hamelers B, Rozendal R, Schröder U, Keller J, Freguia S, Aelterman P, Verstraete W, Rabaey K (2006) Microbial fuel cells: methodology and technology. *Environ Sci Technol* 40:5181–5192
- Mohan SV, Srikanth S, Raghuvulu SV, Mohanakrishna G, Kumar AK, Sarma PN (2009) Evaluation of the potential of various aquatic eco-systems in harnessing bioelectricity through benthic fuel cell: effect of electrode assembly and water characteristics. *Bioresour Technol* 100:2240–2246
- Neumann G, Römheld V (2007) The release of root exudates as affected by the plant physiological status. In: Pinto R, Varanini Z, Nanipieri P (eds) *The rhizosphere. Books in soils, plants, and the environment*. CRC, Boca Raton, pp 23–72
- Pant D, Van Bogaert G, Diels L, Vanbroekhoven K (2010) A review of the substrates used in microbial fuel cells (MFCs) for sustainable energy production. *Bioresour Technol* 101:1533–1543
- Rabaey K, Ossieur W, Verhaege M, Verstraete W (2005) Continuous microbial fuel cells convert carbohydrates to electricity. *Water Sci Technol* 52:515–523
- Read S, Marzorati M, Guimaraes BCM, Boon N (2011) Microbial resource management revisited: successful parameters and new concepts. *Appl Microbiol Biotechnol* 90:861–871
- Reimers CE, Tender LM, Fertig S, Wang W (2001) Harvesting energy from the marine sediment–water interface. *Environ Sci Technol* 35:192–195
- Scott K, Cotlarciuc I, Hall D, Lakeman JB, Browning D (2008) Power from marine sediment fuel cells: the influence of anode material. *J Appl Electrochem* 38:1313–1319
- Strik DPBTB, Hamelers HVM, Snel JFH, Buisman CJN (2008) Green electricity production with living plants and bacteria in a fuel cell. *Int J Energ Res* 32:870–876
- Tender LM, Gray SA, Groveman E, Lowy DA, Kauffman P, Melhado J, Tyce RC, Flynn D, Petrecca R, Dobarro J (2008) The first demonstration of a microbial fuel cell as a viable power supply: powering a meteorological buoy. *J Power Sources* 179:571–575
- Timmers RA, Strik DPBTB, Hamelers HVM, Buisman CJN (2010) Long-term performance of a plant microbial fuel cell with *Spartina anglica*. *Appl Microbiol Biotechnol* 86:973–981
- Tripisciano C, Kozynchenko OP, Linsberger I, Phillips GJ, Howell CA, Sandeman SR, Tennison SR, Mikhailovsky SV, Weber V, Falkenhagen D (2011) Activation-dependent adsorption of cytokines and toxins related to liver failure to carbon beads. *Biomacromolecules* 12:3733–3740
- Williams KH, Nevin KP, Franks A, Englert A, Long PE, Lovley DR (2010) Electrode-based approach for monitoring in situ microbial activity during subsurface bioremediation. *Environ Sci Technol* 44:47–54
- Yuan Y, Zhou SG, Zhuang L (2010) A new approach to in situ sediment remediation based on air-cathode microbial fuel cells. *J Soils Sediments* 10:1427–1433
- Zhang T, Gannon SM, Nevin KP, Franks AE, Lovley DR (2010) Stimulating the anaerobic degradation of aromatic hydrocarbons in contaminated sediments by providing an electrode as the electron acceptor. *Environ Microbiol* 12:1011–1020